UNIVERSIDAD DE INVESTIGACIÓN DE TECNOLOGÍA EXPERIMENTAL YACHAY

Escuela de Ciencias Físicas y Nanotecnología

TÍTULO: Study of the scalar cosmological perturbations up to first order in deviation for the chaotic inflationary model

Trabajo de integración curricular presentado como requisito para la obtención
del título de Físico

Autor:

Tapia Mora Truman

Tutor:

Ph. D. Rojas Cely Clara

Urcuquí, julio 2020

UNIVERSIDAD YACHAY TECH

Urcuquí, 27 de abril de 2020

SECRETARÍA GENERAL
(Vicerrectorado Académico/Cancillería)
ESCUELA DE CIENCIAS FÍSICAS Y NANOTECNOLOGÍA
CARRERA DE FÍSICA
ACTA DE DEFENSA No. UITEY-PHY-2020-00007-AD

A los 27 días del mes de abril de 2020, a las 14:30 horas, de manera virtual mediante videoconferencia, y ante el Tribunal Calificador, integrado por los docentes:

Presidente Tribunal de Defensa	Dr. COSENZA MICELI, MARIO GIUSEPPE , Ph.D.
Miembro No Tutor	Dr. RAMIREZ VELASQUEZ JOSE MANUEL , Ph.D.
Tutor	Dra. ROJAS CELY CLARA INES , Ph.D.

El(la) señor(ita) estudiante **TAPIA MORA, TRUMAN EMANUEL**, con cédula de identidad No. **0603513979**, de la **ESCUELA DE CIENCIAS FÍSICAS Y NANOTECNOLOGÍA**, de la Carrera de **FÍSICA**, aprobada por el Consejo de Educación Superior (CES), mediante Resolución **RPC-SO-39-No.456-2014**, realiza a través de videoconferencia, la sustentación de su trabajo de titulación denominado: **Study of the scalar cosmological perturbations up to first order in deviation for the chaotic inflationary model**, previa a la obtención del título de **FÍSICO/A**.

El citado trabajo de titulación, fue debidamente aprobado por el(los) docente(s):

Tutor	Dra. ROJAS CELY CLARA INES , Ph.D.

Y recibió las observaciones de los otros miembros del Tribunal Calificador, las mismas que han sido incorporadas por el(la) estudiante.

Previamente cumplidos los requisitos legales y reglamentarios, el trabajo de titulación fue sustentado por el(la) estudiante y examinado por los miembros del Tribunal Calificador. Escuchada la sustentación del trabajo de titulación a través de videoconferencia, que integró la exposición de el(la) estudiante sobre el contenido de la misma y las preguntas formuladas por los miembros del Tribunal, se califica la sustentación del trabajo de titulación con las siguientes calificaciones:

Tipo	Docente	Calificación
Miembro Tribunal De Defensa	Dr. RAMIREZ VELASQUEZ JOSE MANUEL , Ph.D.	9,5
Presidente Tribunal De Defensa	Dr. COSENZA MICELI, MARIO GIUSEPPE , Ph.D.	10,0
Tutor	Dra. ROJAS CELY CLARA INES , Ph.D.	9,9

Lo que da un promedio de: **9.8 (Nueve punto Ocho)**, sobre 10 (diez), equivalente a: **APROBADO**

Para constancia de lo actuado, firman los miembros del Tribunal Calificador, el/la estudiante y el/la secretario ad-hoc.

Certifico que *en cumplimiento del Decreto Ejecutivo 1017 de 16 de marzo de 2020, la defensa de trabajo de titulación (o examen de grado modalidad teórico práctica) se realizó vía virtual, por lo que las firmas de los miembros del Tribunal de Defensa de Grado, constan en forma digital.*

TAPIA MORA, TRUMAN EMANUEL
Estudiante

Dr. COSENZA MICELI, MARIO GIUSEPPE , Ph.D.
Presidente Tribunal de Defensa

Firmado electrónicamente por:
MARIO GIUSEPPE
COSENZA MICELI

Dra. ROJAS CELY CLARA INES , Ph.D.
Tutor

Firmado electrónicamente por:
CLARA INES
ROJAS CELY

Dr. RAMIREZ VELASQUEZ JOSE MANUEL , Ph.D.
Miembro No Tutor

Firmado electrónicamente por:
JOSE MANUEL RAMIREZ VELASQUEZ

CIFUENTES TAFUR, EVELYN CAROLINA
Secretario Ad-hoc

Firmado electrónicamente por:
EVELYN CAROLINA CIFUENTES TAFUR

AUTORÍA

Yo, **TRUMAN EMANUEL TAPIA MORA**, con cédula de identidad 0603513979, declaro que las ideas, juicios, valoraciones, interpretaciones, consultas bibliográficas, definiciones y conceptualizaciones expuestas en el presente trabajo; así cómo, los procedimientos y herramientas utilizadas en la investigación, son de absoluta responsabilidad de el/la autora (a) del trabajo de integración curricular. Así mismo, me acojo a los reglamentos internos de la Universidad de Investigación de Tecnología Experimental Yachay.

Urcuquí, julio 2020.

T. Tapia

Truman Emanuel Tapia Mora

CI: 0603513979

AUTORIZACIÓN DE PUBLICACIÓN

Yo, **TRUMAN EMANUEL TAPIA MORA,** con cédula de identidad 0603513979, cedo a la Universidad de Investigación de Tecnología Experimental Yachay, los derechos de publicación de la presente obra, sin que deba haber un reconocimiento económico por este concepto. Declaro además que el texto del presente trabajo de titulación no podrá ser cedido a ninguna empresa editorial para su publicación u otros fines, sin contar previamente con la autorización escrita de la Universidad.

Asimismo, autorizo a la Universidad que realice la digitalización y publicación de este trabajo de integración curricular en el repositorio virtual, de conformidad a lo dispuesto en el Art. 144 de la Ley Orgánica de Educación Superior

Urcuquí, julio 2020.

T. Tapia

Truman Emanuel Tapia Mora

CI: 0603513979

Resumen

La Inflación Cosmológica surgió para resolver los problemas de ajuste fino del modelo clásico del Big Bang. La inflación manifiesta que una expansión exponencial ocurrió en el universo temprano. Con muchos modelos diferentes propuestos, la inflación es aún un campo abierto de estudio. La principal característica para discriminar entre modelos inflacionarios es el espectro de potencias. Este trabajo presenta un cálculo numérico del espectro de potencias escalares para el modelo de inflación caótica $\frac{1}{2}m^2\varphi_0^2$, obteniendo un índice espectral de $n_s = 0.9689$. El índice espectral encontrado concuerda con las últimas mediciones de la inflación.

Palabras Clave: inflación cosmológica, espectro de potencias, numérico.

Abstract

Cosmological Inflation emerged to solve the fine-tuning problems of the classical Big Bang model. Inflation states that an exponential expansion occurred in the early universe. With plenty different proposed models, inflation is still an open field of study. The main characteristic to discriminate between inflationary models is the power spectrum. This work presents a numerical calculation of the power spectrum of scalar perturbations for the chaotic inflationary model $\frac{1}{2}m^2\varphi_0^2$, getting a spectral index of $n_s = 0.9689$. The spectral index found is in good agreement with the latest measurements of inflation.

Key Words: cosmological inflation, power spectrum, numerical.

Contents

List of Figures

List of Tables

Chapter 1

Introduction

The evolution of the Universe has been one of the most intriguing questions to humanity. Since the last century, this question has gone from being speculation to pure science. Prominent developments in science allowed the emergence of the Big Bang theory, such as the foundation of General Relativity by Albert Einstein[2,3], the finding that galaxies are receding away from us, and the idea that the Universe expanded from a single point. The Big Bang theory states that all the content of the Universe was concentrated in a hot, dense, and infinitesimally small point (the singularity). Then, the Universe expanded from the singularity, and while the expansion occurs, the Universe also cools down giving rise to the constituents of the Universe, such as neutrinos, photon, electrons, protons, among others. Nowadays the Big Bang model is the most accepted model of the evolution of the Universe. It is strongly supported by observations, such as the measurements of the Cosmic Microwave Background (CMB)[4], the expansion of the Universe, and the abundances of light elements in the Universe. However, the Big Bang model presents some weak points as the "Fine-Tuning problems". These problems state that the existence of the current Universe requires some extremely fine tuned initial conditions. Motivated to solve the fine-tuning problems Alan Guth discovered Cosmological Inflation[5], a theory for the dynamics of the early Universe.

Inflation was born in 1980 as a solution to the fine-tuning problems. This theory states that in the very early Universe there was a huge expansion. Also, a great virtue of inflation is that it provides a natural way of explaining the CMB anisotropies and the large scale structure of the Universe through the growing of quantum vacuum fluctuations[6 7]. Plenty of different inflationary models have been proposed[8], each one with a different motivation and underlying physics. Currently, testing the validity of each model is an active area of research inside inflation. This test is done comparing the predicted power spectrum of each inflationary model with measurements of CMB anisotropies[1 9 10]. The present work is oriented to provide a code to calculate numerically the power spectrum of scalar perturbation for a chaotic inflationary model, so that future works could extend this code to include more models of inflation.

1.1 Summary of the Big Bang theory

Inflation is an extension to the classical Big Bang model, then it is indispensable to start discussing general aspects of this theory. The cornerstone of Cosmology is the cosmological principle, which states that at large scales the Universe is homogeneous and isotropic. In other words, the Universe is the same everywhere and in all directions. An expanding (or contracting) Universe which obeys the cosmological principle is described by the Friedmann-Lamaıtre-Robertson-Walker (FLRW) metric

$$\mathrm{d}s^2 = -\mathrm{d}t^2 + a^2(t)\left[\frac{\mathrm{d}r^2}{1-Kr^2} + r^2\left(\mathrm{d}\theta^2 + \sin^2\theta\mathrm{d}\phi^2\right)\right], \tag{1.1}$$

where the constant K describes the curvature of the Universe. The coordinates t, r, θ, and ϕ are comoving coordinates. The variable a is the scale factor, which describes the expansion of the Universe. The relationship between physical and comoving distances is

$$x(t) = a(t)r, \tag{1.2}$$

where x represents a physical distance. The dynamics of the Universe is calculated by solving the Einstein Field Equations:

$$G_{\mu\nu} + \Lambda g_{\mu\nu} = 8\pi G \ T_{\mu\nu}. \tag{1.3}$$

In the last expression $c = 1$, G is the universal gravitational constant, $g_{\mu\nu}$ stands for the metric tensor, and $G_{\mu\nu}$ is the Einstein tensor. The cosmological constant Λ plays the role of dark energy. $T_{\mu\nu}$ is the energy-momentum tensor which describes the content of the Universe. The left hand side of this equation is constructed from the line element (1.1) (detailed formulas are presented in Section 2.3.1). The energy-momentum tensor for a Universe filled of N perfect fluids is:

$$T_{\mu\nu} = \sum_{i=1}^{i=N} T^{(i)}_{\mu\nu} = \sum_{i=1}^{i=N} \left\{ \left[\rho_i(t) + p_i(t)\right] u_\mu u_\nu + p_i(t) g_{\mu\nu} \right\}, \tag{1.4}$$

where p_i and ρ_i are the pressure and density of the i perfect fluid, respectively. The vector u_μ is a four velocity in comoving coordinates given by $u = (1, 0, 0, 0)$. To solve the Einstein equations, it is important to consider the equation of state given by $p_i = w_i \rho_i$. Then, with these considerations, the equations that follow from Einstein Field Equations are

$$\frac{\ddot{a}}{a} = -\frac{4\pi G}{3} \sum_{i=1}^{N} (\rho_i + 3p_i) + \frac{1}{3}\Lambda, \tag{1.5}$$

$$\frac{\dot{a}^2}{a^2} + \frac{K}{a^2} = \frac{8\pi G}{3} \sum_{i=1}^{N} \rho_i + \frac{\Lambda}{3}, \tag{1.6}$$

where dots above the variables represent differentiation with respect to time. Equations (1.5) and (1.6) can be simplified through several approximations to get analytical solutions. First, it is assumed that the Universe is mainly filled with just one fluid with constant equation of state per epoch. Second, we can assume a vanishing cosmological constant for the purpose of inflation.

Third, the curvature of the Universe $K = 0$ as current measurements suggest[11]. Thus, we get the acceleration equation

$$\frac{\ddot{a}}{a} = -\frac{4\pi G}{3}\left(\rho + 3p\right), \tag{1.7}$$

and the Friedman equation,

$$\left(\frac{\dot{a}}{a}\right)^2 = H^2 = \frac{8\pi G}{3}\rho, \tag{1.8}$$

where $H = \dot{a}/a$ is the Hubble parameter. Also, we use the conservation of the energy-momentum tensor $T^{\mu\nu}_{;\nu} = 0$ to find the continuity equation

$$\dot{\rho} + 3H(\rho + p) = 0. \tag{1.9}$$

The solution of (1.9) leads to the dynamics of the density

$$\rho(t) = \rho_{\mathrm{f}}\left(\frac{a_{\mathrm{f}}}{a}\right)^{3(1+w)}, \tag{1.10}$$

where the constant $\rho_{\mathrm{f}} = \rho\left(t_{\mathrm{f}}\right)$ can be change to any useful time. Then, substituting this result in (1.8) gives

$$\left(\frac{\dot{a}}{a}\right)^2 = \frac{8\pi G\rho_{\mathrm{f}}}{3}\left(\frac{a_{\mathrm{f}}}{a}\right)^{3(1+w)}, \tag{1.11}$$

and solving this we get the scale factor

$$\left[\frac{a(t)}{a_{\mathrm{f}}}\right]^{\frac{3(1+w)}{2}} = \frac{3(1+w)}{2}\rho_{\mathrm{f}}^{1/2}\left(\frac{8\pi G}{3}\right)^{1/2} t + C, \tag{1.12}$$

where C is a integration constant. Requiring that $a(t_f) = a_f$ and using (1.8), we find that the scale factor is given by

$$a(t) = a_\mathrm{f}\left[\frac{3}{2}(1+w)H_\mathrm{f}\left(t-t_\mathrm{f}\right)+1\right]^{\frac{2}{3(1+w)}}. \tag{1.13}$$

In this equation, if $t = t_\mathrm{BB} = t_\mathrm{f} - 2/\left[3(1+w)H_\mathrm{f}\right]$, the scale factor is zero. It is meaningless to consider times when $t < t_\mathrm{BB}$, in this sense t_BB is the beginning of time when the Big Bang starts. We can write equation (1.13) in terms of t_{BB} and fix $t_{BB} = 0$, finding an equation for the scale factor in the form

$$a(t) = a_\mathrm{f}\left(\frac{t}{t_\mathrm{f}}\right)^{\frac{2}{3(1+w)}}. \tag{1.14}$$

This equation gives simple expressions for the scale factor in different epochs of the Universe. The whole history of the Universe can be divided in three epochs. Inside each epoch the Universe is mainly filled with just one constituent. The transition from one epoch to another must be smooth, so that a and H must be continuous at the time of transition. In the first epoch the Universe is filled with radiation, described by an equation of state $w = 1/3$, then the scale factor is $a \propto t^{1/2}$. Second, an epoch dominated by matter, described by an equation of state $w = 0$, then $a \propto t^{2/3}$. Third, an epoch dominated by dark energy, described by $w = -1$, in this case the scale factor is ill defined, which corresponds to the exponential expansion $a(t) = a_\mathrm{f} \exp\left[H_\mathrm{f}\left(t - t_\mathrm{f}\right)\right]$.

1.2 Fine-Tuning Problems

Among the several fine-tuning problems, then the horizon and flatness problems are described following the ideas presented by Martin[12].

1.2.1 Horizon Problem

According to the classical Big Bang model the CMB is formed of plenty of causally disconnected regions, then they could never exchange heat or information, but measurements show that the

CMB has the same temperature everywhere. The Big Bang model can not explain this fact, the homogeneity in temperature must be consider an initial condition of the Universe. To take a closer look of this problem, consider the size of a causally connected sphere on the CMB. First, CMB was set when radiation decoupled from matter at the last scattering surface. For the purpose in hand, consider that this event occurred in the time when radiation and matter were in equilibrium t_{eq}. The angular size of a causally connected sphere on the CMB is:

$$\delta\theta = \int_0^{t_{eq}} \frac{dt'}{a(t')} \left[\int_{t_{eq}}^{t_o} \frac{dt'}{a(t')} \right]^{-1} . \tag{1.15}$$

The integral on the numerator represents the size of the causally connected sphere, and on the denominator is the distance from the CMB to the Earth. These integrals are solved using the piece-wise behavior of the scale factor discussed at the end of section 1.1, but considering that the Universe just had a radiation epoch followed by a matter epoch (considering a dark energy epoch would make the problem even more severe). The transition from radiation to matter occurs at t_{eq}, then the integral on the numerator just handles a radiation scale factor, and the denominator just handles a matter epoch. Starting with the denominator the scale factor is $a(t) = a_{eq}[(3/2)H_{eq}(t - t_{eq}) + 1]^{2/3}$ following (1.13), and the integral is

$$\begin{aligned} \int_{t_{eq}}^{t_o} \frac{dt'}{a(t')} &= \frac{1}{a_{eq}} \int_{t_{eq}}^{t_o} dt' \left[(3/2)H_{eq}(t' - t_{eq}) + 1 \right]^{-2/3} , \\ &= \frac{2}{a_{eq}H_{eq}} \left[\left(\frac{a(t')}{a_{eq}} \right)^{1/2} \right]_{t_{eq}}^{t_o} = \frac{2}{a_{eq}H_{eq}} \left[\left(\frac{a_o}{a_{eq}} \right)^{1/2} - 1 \right], \end{aligned} \tag{1.16}$$

The Hubble parameter during this epoch can be rewritten as $H = a_{eq}^{3/2} H_{eq} a^{-3/2}$. Using this we find that

$$\frac{1}{a_{eq}H_{eq}} = \frac{1}{a_o H_o} \frac{a_o H_o}{a_{eq}H_{eq}} = \frac{1}{a_o H_o} \frac{a_o a_{eq}^{3/2} a_o^{-3/2} H_{eq}}{a_d H_{eq}} = \frac{1}{a_o H_o} \left(\frac{a_{eq}}{a_o} \right)^{1/2} , \tag{1.17}$$

and replacing this in (1.16) gives

$$\int_{t_{eq}}^{t_o} \frac{dt'}{a(t')} = \frac{2}{a_o H_o}\left[1 - \left(\frac{a_{eq}}{a_o}\right)^{1/2}\right]. \tag{1.18}$$

The integral on the numerator uses the scale factor $a(t) = a_{eq}(2H_{eq}t)^{1/2}$ following (1.14), and the integral is

$$\begin{aligned}\int_0^{t_{eq}} \frac{dt'}{a(t')} &= \frac{1}{a_{eq}\sqrt{2H_{eq}}}\int_0^{t_{eq}} \frac{dt'}{\sqrt{t'}} = \left[\frac{\sqrt{2t'}}{a_{eq}\sqrt{H_{eq}}}\right]_0^{t_{eq}} \\ &= \left[\frac{1}{a_{eq}\sqrt{H(t')H_{eq}}}\right]_0^{t_{eq}} = \frac{1}{H_{eq}a_{eq}}.\end{aligned} \tag{1.19}$$

Using equation (1.17) in the last result gives

$$\int_0^{t_{eq}} \frac{dt'}{a(t')} = \frac{1}{a_o H_o}\left(\frac{a_{eq}}{a_o}\right)^{1/2}, \tag{1.20}$$

Finally, replacing the results of the two integrals in $\delta\theta$, and using the definition of redshift $z(t) = \frac{a_o}{a(t)} - 1$ we find that

$$\delta\theta = \frac{1}{2}\left(\sqrt{z_{eq} + 1} - 1\right)^{-1}. \tag{1.21}$$

Considering that the redshift of the radiation decoupling event is $z_{eq} = 1089$, the last result gives $\delta\theta \approx 0.0156$. This means that scales larger than 0.89° on the CMB were not causally connected. Thus, the CMB should be filled of plenty of patches with different temperatures (unless homogeneity is considered as initial condition), but this is not the case. Measurements show that temperature of the CMB is very isotropic, and anisotropies just appear in the order of 10^{-5}.

1.2.2 Flatness Problem

To study the flatness problem, we have to consider the dynamics of the curvature of the Universe. If cosmological constant is neglected, equation (1.6) can be rewritten as

$$1 + \frac{K}{a^2H^2} = \Omega_T, \tag{1.22}$$

where

$$\Omega_T = \sum_i \Omega_i = \sum_i \frac{\rho_i}{\rho_{cri}} \quad ; \quad \rho_{cri} = \frac{3H^2}{8\pi G}. \tag{1.23}$$

If $\Omega_T = 1$, then $K = 0$, which means that the Universe will be flat. Current measurements suggest that the Universe is close to be flat. Using (1.10), Ω_T can be rewritten as:

$$\begin{aligned} \Omega_T &= \frac{1}{\rho_{cri}} \sum_i \rho_i^o \Big(\frac{a_o}{a}\Big)^{3(1+w_i)} \\ &= \frac{H_o^2}{H^2} \sum_i \Omega_i^o \Big(\frac{a_o}{a}\Big)^{3(1+w_i)}, \end{aligned} \tag{1.24}$$

where superscript o means that the variable is evaluated at present time. Also, using equation (1.22) for an approximately flat Universe, we get that

$$\Omega_T - 1 = \left(\frac{H_o}{H}\right)^2 (\Omega_T^o - 1) \left(\frac{a_o}{a}\right)^2. \tag{1.25}$$

Combining equations (1.24) and (1.25) we can find that

$$\Omega_T(t) = \frac{\sum_i \Omega_i^o \left(\frac{a_o}{a}\right)^{3(1+w_i)}}{\sum_i \Omega_i^o \left(\frac{a_o}{a}\right)^{3(1+w_i)} - (\Omega_T^o - 1)\left(\frac{a_o}{a}\right)^2}, \tag{1.26}$$

and considering just radiation and matter epochs the summation in this equation turns in

$$\Omega_T(t) = \frac{\Omega_m^o\left(\frac{a_o}{a}\right) + \Omega_{rad}^o\left(\frac{a_o}{a}\right)^2}{\Omega_m^o\left(\frac{a_o}{a}\right) + \Omega_{rad}^o\left(\frac{a_o}{a}\right)^2 - (\Omega_T^o - 1)} = \left(1 - \frac{(\Omega_T^o - 1)a^2/a_o}{a\Omega_m^o + a_o\Omega_{rad}^o}\right)^{-1}. \tag{1.27}$$

Finally, doing a Taylor expansion and rearranging we get:

$$\Omega_T(t) = 1 + \frac{\left(\Omega_T^o - 1\right)a_o(z+1)^{-2}}{a\Omega_m^o + a_o\Omega_{rad}^o},$$
$$\Omega_T^o - 1 = (\Omega_T(z) - 1)\left[(z+1)\Omega_m^o + (z+1)^2\Omega_{rad}^o\right]. \tag{1.28}$$

Planck mission 2018[11] reported $|\Omega_T^o - 1| \lesssim 0.003$, $\Omega_{rad}^o \approx 9.159 \times 10^{-5}$, and $\Omega_m^o \approx 0.315$. The last expression shows the flatness problem, as we go back in time (namely increase z), $\Omega_T(z) - 1$ must be lower and lower to keep the equality. For example, going back to the time of Big Bang Nucleosynthesis (BBN) with $z_{BBN} \approx 10^8$, $|\Omega_T(z_{BBN}) - 1| \lesssim 10^{-15}$, and this value turns even lower as we go back in time. We see that in the classical Big Bang model the curvature of the Universe is extremely fine tuned, which is a very unlikely condition. Therefore, a new mechanism is required to circumvent the fine-tuning problems, and the most accepted solution is Cosmological Inflation. But as was discussed earlier, this theory is not completely developed, for example many models of inflation have been proposed. To prove each model, the calculation of the power spectrum of perturbations is a key part.

1.3 General and Specific Objectives

The main objective of this work is to calculate numerically the power spectrum of scalar perturbations for the chaotic inflationary model $\frac{1}{2}m^2\varphi_0^2$. In Chapter 2, the theoretical backgrounds required are discussed, starting with the definition of inflation, and how the dynamics of the

Universe behaves during this epoch. Also, the solution to the fine-tuning problems is developed. Then, the slow-roll approximation of inflation is introduced. The first order scalar cosmological perturbations are discussed at the middle of this chapter, and the chaotic inflationary model is presented at the end of this chapter. In Chapter 3, the results of this work are presented. First the results of background dynamics are presented. Second, the solutions to the Mukhanov-Sasaki equation are presented together with the results of the curvature perturbation. Third, the full power spectrum of scalar perturbations is presented with its respective spectral index and running. The last Chapter 4 contains a summary of the work, and future research projects that could develop from this work.

In the following work, the Einstein summation convention is used. As usual, greek indices run from 0 to 3, and latin indexes run from 1 to 3. The signature of the metric employed is $(-,+,+,+)$. The symbol $\dot{}$ denotes differentiation with respect to cosmic time t, and $'$ denotes differentiation with respect to the conformal time η. It is possible to go from time to conformal time using $dt = a\mathrm{d}\eta$. Also, $\hbar$ and c are set to 1, and the reduced Planck mass defined as $M_{\mathrm{Pl}} = (8\pi G)^{-1/2}$ is used.

Chapter 2

Methodology

2.1 Inflation

Strictly speaking, the horizon and flatness problems do not break the classical Big Bang theory. They can be overcome just assuming that initially the Universe had the same temperature everywhere and was extremely flat, but these conditions are really unlikely. Cosmological Inflation provides a logic way to solve the fine-tuning problems. Inflation can be defined as an epoch when the Universe has an accelerated expansion, hence the scale scale factor obeys that [13]

$$\ddot{a} > 0. \tag{2.1}$$

Using this definition with the equation (1.7) gives the condition

$$\rho + 3P < 0. \tag{2.2}$$

Because the density must be positive, the "exotic matter" driving inflation must have a negative pressure. Also, equation (2.1) can be rewritten to give a more illustrative condition for inflation:

$$\frac{d}{dt}\frac{H^{-1}}{a} < 0, \tag{2.3}$$

where $(Ha)^{-1}$ is called the Hubble length, Hubble horizon, or simply horizon in comoving reference frame (using $c = 1$). Beyond the horizon objects are receding with a speed faster than the speed of light[14]. Also, while the Universe expands appreciably (e.g. inflation), the horizon gives a good estimate of the observable Universe. From the last condition, inflation can be defined as any epoch where the observable Universe, viewed in coordinates fixed with the expansion, is decreasing. It is important to quantify how much the Universe expands during this epoch, because of the large numbers managed during inflation, this is quantify with the number of e-foldings N. The number of e-foldings from a initial time t_i to a time t is given by

$$N(t) = ln\left[\frac{a(t)}{a(t_i)}\right]. \tag{2.4}$$

CMB measurements suggest that inflation takes place near the Grand Unify Theory energy scale, hence to model this epoch usually field theory is employed. Inflationary models described with a single scalar field are strongly favored by current measurements[1]. Following these type of models, the energy density and pressure for a Universe containing a single scalar field are:

$$\rho = \frac{1}{2}\dot{\varphi}^2 + V(\varphi), \tag{2.5}$$

$$p = \frac{1}{2}\dot{\varphi}^2 - V(\varphi), \tag{2.6}$$

where φ is a scalar field usually called inflaton, and $V(\varphi)$ is a potential which depends on the model of inflation. These two result follow from the definition (2.35). Considering (2.6), if the potential dominates over the kinetic energy, the pressure becomes negative, whence fulfilling the condition (2.2) to have inflation. Replacing the last two equations in (1.7), (1.8), and (1.9) gives the equations of motion of the Universe during inflation

$$\frac{\ddot{a}}{a} = -\frac{8\pi G}{3}\left[\dot{\varphi}^2 - V(\varphi)\right], \tag{2.7}$$

$$H^2 = \frac{8\pi G}{3}\left[V(\varphi) + \frac{1}{2}\dot{\varphi}^2\right], \tag{2.8}$$

$$\ddot{\varphi} + 3H\dot{\varphi} + V_{,\varphi} = 0, \tag{2.9}$$

where "$_{,\varphi}$" means differentiation with respect to φ. A useful relation that is going to be used in the following calculations is found by differentiating (2.8) with respect to time:

$$2H\dot{H} = l^2\left(\dot{\varphi}\ddot{\varphi} + V_{,\varphi}\,\dot{\varphi}\right), \tag{2.10}$$

and then adding this to the equation $l^2\dot{\varphi}(\ddot{\varphi} + 3H\dot{\varphi} + V_{,\varphi}) = 0$, which comes from (2.9), gives

$$\dot{H} = -\frac{3}{2}l^2\dot{\varphi}^2, \tag{2.11}$$

or in conformal time

$$\mathcal{H}^2 - \mathcal{H}' = \frac{3}{2}l^2\varphi'^2, \tag{2.12}$$

where the definition $\mathcal{H} = \frac{a'}{a}$ is used.

2.1.1 Inflation and the Horizon problem

We shall consider adding an epoch of inflation to the description of the Universe of Section 1.2.1, and see how this new epoch solves the horizon problem. Inflation is going to occur inside the radiation era; it starts at t_i, and ends at t_{end}. With these considerations, the angular size of the causally connected sphere (1.15) is

$$\delta\theta = \left[\int_0^{t_i}\frac{dt'}{a(t')} + \int_{t_i}^{t_{end}}\frac{dt'}{a(t')} + \int_{t_{end}}^{t_{eq}}\frac{dt'}{a(t')}\right]\left[\int_{t_{eq}}^{t_o}\frac{dt'}{a(t')}\right]^{-1}. \tag{2.13}$$

The first and last integrals in the numerator will give a small contribution as seen in the horizon problem, so $\delta\theta$ can be approximated as

$$\delta\theta = \left[\int_{t_i}^{t_{end}} \frac{d\tau}{a(\tau)}\right]\left[\int_{t_d}^{t_o} \frac{d\tau}{a(\tau)}\right]^{-1}. \tag{2.14}$$

To calculate the integral in the numerator we consider a phase of inflation with a scale factor following (1.13),
$a = a_i\left[\frac{3}{2}(1+w)H_i(t-t_i)+1\right]^{\frac{2}{3(1+w)}}$, with this prescription the integral is

$$\begin{aligned}\int_{t_i}^{t_{end}} \frac{dt'}{a(t')} &= \frac{1}{a_i}\int_{t_i}^{t_{end}}\left[\frac{3}{2}(1+w)H_i(t'-t_i)+1\right]^{-\frac{2}{3(1+w)}} \\ &= \left[\frac{2}{(1+3w)H(t')a(t')}\right]_{t_i}^{t_{end}} = \frac{2}{1+3w}\left(\frac{1}{a_{end}H_{end}} - \frac{1}{a_iH_i}\right).\end{aligned} \tag{2.15}$$

Using the fact that the Hubble parameter can be written as $H(t) = H_i(a_i/a)^{3(w+1)/2}$ during inflation, the last result takes the form:

$$\int_{t_i}^{t_{end}} \frac{dt'}{a(t')} = \frac{2}{a_iH_i(1+3w)}\left[\left(\frac{a_{end}}{a_i}\right)^{\frac{1+3w}{2}} - 1\right]. \tag{2.16}$$

Also, doing the same procedure as in equation (1.17) we get that

$$\frac{1}{a_iH_i} = \frac{1}{a_oH_o}\frac{a_i^{(1+3w)/2}}{a_o^{1/2}a_{eq}^{1/2}a_{end}^{(3w-1)/2}}, \tag{2.17}$$

then equation (2.16) turns in

$$\int_{t_i}^{t_{end}} \frac{dt'}{a(t')} = \frac{2}{a_oH_o(1+3w)}\frac{a_{end}}{a_o^{1/2}a_{eq}^{1/2}}\left[1 - \left(\frac{a_i}{a_{end}}\right)^{\frac{1+3w}{2}}\right]. \tag{2.18}$$

Using this result we can calculate the angular size (2.14). To solve the horizon problem we impose that $\delta\theta \geq 2\pi$, which gives the expression

$$\delta\theta = \frac{a_{end}}{a_o^{1/2} a_{eq}^{1/2} - a_{eq}} \frac{1}{(1+3w)} \left[1 - e^{-\frac{N_T}{2}(1+3w)}\right] \geq 2\pi, \tag{2.19}$$

where N_T is the total number e-foldings during inflation. Solving for N_T we get that

$$N_T \gtrsim \frac{-2}{1+3w} \ln\left[\frac{-2\pi(1+3w)}{z_{eq}+1}\left(\sqrt{z_{eq}+1} - 1\right)(z_{end}+1)\right]. \tag{2.20}$$

This result gives the number of e-foldings required to solve the horizon problem. To put some numbers in the last result, consider that inflation occurs near the Grand Unified Theory (GUT) scale, then $z_{end} \approx 10^{27}$[12]. Setting $w \approx -1$, and $z_{eq} = 1089$; we get that $N_T \gtrsim 60$. Thus, the horizon problem is solved if inflation can provide at least 60 e-foldings. Notice that the parameters z_{end} and w can be relaxed and inflation still will solve the horizon problem.

2.1.2 Inflation and the Flatness problem

We are going to add an epoch of inflation to the description of the flatness problem, and see how this procedure can solve the problem. Consider equation (1.28) with an added epoch of inflation going from t_i to t_{end}. The furthest possible redshift that can be reached in this equation is z_{end}, because this equation is based in the classical Big Bang model. For this reason, it is useful to find z_{end} in terms of z_i to study the impact of inflation. Similar to equation (1.27), we can find that

$$\begin{aligned} \Omega_T(t) &= \frac{\Omega_x^i \left(\frac{a_i}{a}\right)^{3(1+w_i)}}{\Omega_x^i \left(\frac{a_i}{a}\right)^{3(1+w_i)} - (\Omega_T^i - 1)\left(\frac{a_i}{a}\right)^2}, \\ \Omega_T(t) &= 1 + \frac{\Omega_T^i - 1}{\Omega_x^i} e^{N_T(1+3w)}, \end{aligned} \tag{2.21}$$

where x represents the matter that drives inflation. Using this result and equation (1.28), we get the condition to solve the flatness problem

$$\Omega_T^o - 1 = \frac{\Omega_T^i - 1}{\Omega_x^i} e^{-N_T(1+3w)} \left[(z_{end}+1)\Omega_m^o + (z_{end}+1)^2 \Omega_{rad}^o\right] \lesssim 0.003. \tag{2.22}$$

Assuming that $\Omega_T^i \approx \Omega_T^o$, namely no fine-tuning, we can find the expression:

$$N \gtrsim \frac{-1}{1+3w} \ln\left[(z_{end}+1)\Omega_m^o + (z_{end}+1)^2\Omega_{rad}^o\right]. \tag{2.23}$$

This result gives the number of e-foldings required to solve flatness problem. Considering that $w \approx -1$ and $z_{end} \approx 10 \times 10^{27}$ (as in the horizon problem), we get that $N \gtrsim 60$. Thus, the flatness problem can be solved without applying any fine-tuning if inflation provides at least 60 e-foldings. Notice that this result agrees with the solution of the horizon problem.

2.2 Slow-roll Approximation

Slow-roll is an approximation that simplifies the equations of motion of the Universe during inflation. The approximation assumes that the kinetic term of the inflaton field is small compared with the potential term. The dynamics of the inflaton dictated by a potential is analogous to the fall of a ball in a bowl (see Figure 2.1), in this case slow-roll approximation is valid as long as the ball is rolling slowly.

Using this approximation the last and first terms of equations (2.8) and (2.9) respectively can be neglected, remaining

$$H^2 = \frac{8\pi G}{3}\left[V(\varphi)\right], \tag{2.24}$$

$$3H\dot{\varphi} = -V_{,\varphi}. \tag{2.25}$$

It is useful to define the slow-roll parameters as

$$\epsilon \equiv \frac{1}{16\pi G}\left(\frac{V'}{V}\right)^2, \tag{2.26}$$

$$\eta \equiv \frac{1}{8\pi G}\frac{V''}{V}, \tag{2.27}$$

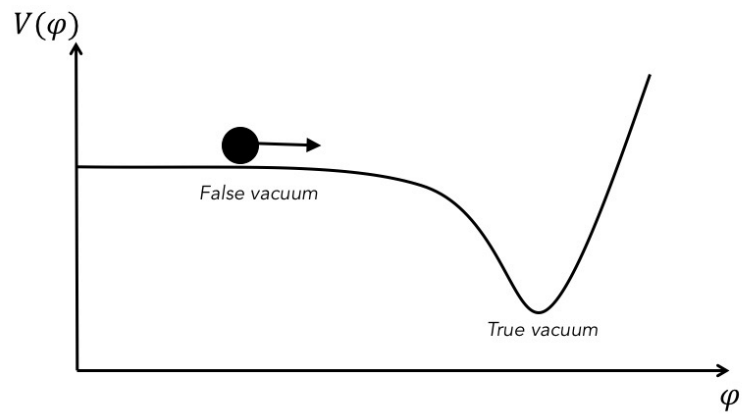

Figure 2.1: Illustration of the dynamics of inflaton φ during slow-roll inflation. Inflation begins when the inflaton field rolls down its potential from a false vacuum to a true vacuum. Image extracted from[15].

$$\delta \equiv \eta - \epsilon, \tag{2.28}$$

and the slow-roll approximation is valid while

$$\epsilon \ll 1, \quad |\eta| \ll 1. \tag{2.29}$$

The first slow-roll parameter ϵ describes the slope of the potential, while the second parameter η describes the curvature of the potential. Using the slow-roll approximation it is possible to rewrite (2.7) as

$$\frac{\ddot{a}}{a} = H^2(1 - \epsilon). \tag{2.30}$$

Considering this equation and recalling the condition (2.1), we find that inflation occurs as long as $\epsilon < 1$. Thus, if slow-roll conditions (2.29) are satisfied, then inflation can occur.

2.3 Cosmological Perturbations

The theory of Cosmological Perturbations combined with Inflation produces a natural and elegant way to explain the large scale structure of the Universe. During inflation, the horizon is going to remain approximately constant, while any physical length will be stretched beyond the horizon (See Figure 2.2). Inflation states that vacuum fluctuations (or small physical lengths) are stretched to macroscopic levels where they will become perturbations of the space-time. After inflation ends, these perturbations will be the seeds of the structure of the Universe growing by gravitational instability.

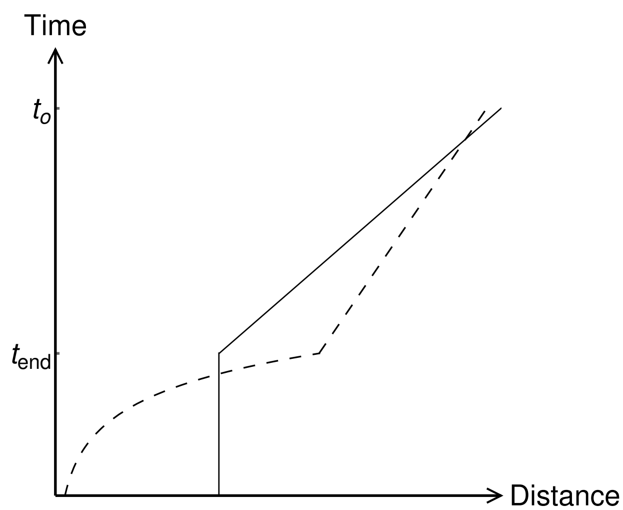

Figure 2.2: Sketch showing the evolution of the horizon (solid curve) and a small physical length (dashed curve). In the time scale, inflation starts at the beginning of the axis and ends in t_{end}, after inflation a period dominated by radiation starts. During an exponential expansion the horizon remains constant, but it increases in the radiation era. The small physical length is stretched during inflation, but expands slower than the horizon in the radiation era. The points where the curves crosses correspond with the times when the physical length leaves and enters the horizon.

2.3.1 Classical Cosmological Perturbations

Classically, cosmological perturbations are studied through General Relativity. To start, the perturbations in any homogeneous tensor are of the form

$$\mathbf{T}(\tau, \mathbf{x}) \equiv \mathbf{T}^{(0)}(\tau) + \delta\mathbf{T}(\tau, \mathbf{x}), \tag{2.31}$$

where $\mathbf{T}^{(0)}$ is the background tensor, and $\delta\mathbf{T}$ is the perturbation. The perturbation can be of any order

$$\delta\mathbf{T}(\tau, \mathbf{x}) \equiv \sum_{n} \frac{\epsilon^n}{n!}\delta_n\mathbf{T}(\tau, \mathbf{x}), \tag{2.32}$$

but in general just the first orders of perturbations are consider because ϵ is small. In the following calculations just first order perturbations are considered, and the parameter ϵ is absorb in the definition of δ_n. The Einstein equations can be splitted as

$$G^{(0)}_{\mu\nu} + \delta G_{\mu\nu} = 8\pi G\left[T^{(0)}_{\mu\nu} + \delta T_{\mu\nu}\right], \tag{2.33}$$

and because the background parts already fulfil the Einstein equations, we get an equation just for perturbations

$$\delta G_{\mu\nu} = 8\pi G\delta T_{\mu\nu}. \tag{2.34}$$

Finding the explicit components of this equation will determine the evolution of the perturbations (in a classical view).

The Energy-Momentum tensor

To start with the right hand side of (2.34), the energy-momentum tensor for a Universe filled with a single scalar field minimally coupled to gravity is given by

$$T^{\mu}_{\nu} = \partial^{\mu}\varphi\partial_{\nu}\varphi - \left[\frac{1}{2}\partial^{\alpha}\varphi\partial_{\alpha}\varphi + V(\varphi)\right]\delta^{\mu}_{\nu}. \tag{2.35}$$

As in equation (2.31) perturbations in the inflaton scalar field can be written in the form

$$\varphi(t,\mathbf{x}) = \varphi_0(t) + \delta\varphi(t,\mathbf{x}). \tag{2.36}$$

Also, the potential is expanded around the background using Taylor expansion as

$$V(\varphi) = V(\varphi_0) + \delta\varphi V_{,\varphi}\,. \tag{2.37}$$

With these considerations and neglecting the background terms we find that

$$\begin{aligned}
\delta T^0_0 &= a^{-2}\left(\Phi\varphi_0'^2 - \varphi_0'\delta\varphi' - a^2\delta\varphi V_{,\varphi}\right), \\
\delta T^0_i &= -a^{-1}\varphi_0'\delta\varphi_{,i}\,, \\
\delta T^i_j &= \delta_{ij}a^{-2}\left[-\Phi(\varphi_0^{'})^2 + \varphi_0^{'}\delta\varphi^{'} - a^2\delta\varphi V_{,\varphi}\right].
\end{aligned} \tag{2.38}$$

The metric

The starting point to determine the left hand side of (2.34) is the metric. Cosmological perturbations in the metric can be decomposed in three types scalar, vector, and tensor perturbations. These three type of perturbations evolve independently at linear order. Vector perturbations have just vanishing solutions, for this reason its study is not relevant. Tensor perturbations result in gravitational waves production, these do not couple to the matter, hence they are not relevant in structure formation (at least in linear order). Scalar perturbations cause perturbations in the space-time and are the seeds for the large scale structure of the Universe. In this work just scalar perturbations are considered. Also, it is important to work with gauge invariant variables (i.e variables that do not depend on a specific coordinate system) because these are the only ones with physical meaning. A straightforward way to achieve this is to work in the longitudinal gauge

(also called conformal Newtonian gauge), which coincides with the gauge invariant Bardeen potentials Ψ and Φ[16]. The variable Ψ is the curvature perturbation and Φ is the gravitational potential. With these prescriptions the line element considering only scalar perturbations in the longitudinal gauge takes the form (for further information about the decomposition of the metric and gauge fixing see[17 18])

$$\mathrm{d}s^2 = -(1+2\Phi)\,\mathrm{d}t^2 + a^2(1-2\Psi)\,\delta_{ij}\mathrm{d}x^i\mathrm{d}x^j, \tag{2.39}$$

and the full metric tensor is

$$g_{\mu\nu} = \begin{pmatrix} -1-2\Phi(t,\mathbf{x}) & 0 & 0 & 0 \\ 0 & a^2[1-2\Psi(t,\mathbf{x})] & 0 & 0 \\ 0 & 0 & a^2[1-2\Psi(t,\mathbf{x})] & 0 \\ 0 & 0 & 0 & a^2[1-2\Psi(t,\mathbf{x})] \end{pmatrix}. \tag{2.40}$$

As the covariant metric $g_{\mu\nu}$ is a diagonal matrix, the contravariant metric $g^{\mu\nu}$ is given by the inverse of each component

$$g^{00} = -\frac{1}{1+2\Phi} \sim -1+2\Phi. \tag{2.41}$$

$$g^{ii} = -\frac{1}{a^2(1-2\Psi)} \sim \frac{1}{a^2}(1+2\Psi). \tag{2.42}$$

Christoffel Symbols

To proceed with the calculation of the perturbed Einstein tensor, the Crisstoffel symbols are computed. The definition of Christoffel symbol is

$$\Gamma^{\mu}_{\alpha\beta} = \frac{1}{2}g^{\mu\nu}\left(g_{\mu\nu,\beta} + g_{\mu\nu,\alpha} - g_{\alpha\beta,\nu}\right), \tag{2.43}$$

and the resulting Christoffel symbols following from the metric (2.40) are

$$
\begin{aligned}
\Gamma^0_{00} &= \dot{\Phi} \\
\Gamma^0_{0i} &= \Phi_{,i}\,, \\
\Gamma^0_{ij} &= \delta_{ij} a^2 [H - 2H(\Psi + \Phi) - \dot{\Psi}], \\
\Gamma^i_{00} &= a^{-2}\Phi_{,i}\,, \\
\Gamma^i_{j0} &= \delta_{ij}(H - \dot{\Psi}), \\
\Gamma^i_{jk} &= -\delta_{ij}\Psi_{,k} - \delta_{ik}\Psi_{,j} + \delta_{jk}\Psi_{,i}\,.
\end{aligned}
\tag{2.44}
$$

The Ricci tensor

The Ricci tensor is defined as

$$
R_{\beta\nu} = \Gamma^{\mu}_{\beta\nu,\mu} - \Gamma^{\mu}_{\beta\mu,\nu} + \Gamma^{\mu}_{\sigma\mu}\Gamma^{\sigma}_{\beta\nu} - \Gamma^{\mu}_{\sigma\nu}\Gamma^{\sigma}_{\beta\mu}, \tag{2.45}
$$

and the resulting Ricci tensor is

$$
\begin{aligned}
R_{00} &= a^{-2}\left[-3\mathcal{H}' + \nabla^2\Phi + 3\Psi'' + 3\mathcal{H}\left(\Phi' + \Psi'\right)\right], \\
R_{0i} &= 2a^{-1}\left(\Psi'_{,i} + \mathcal{H}\Phi_{,i}\right), \\
R_{ij} &= \delta_{ij}\left\{\nabla^2\Psi - \Psi'' + [1 - 2(\Phi + \Psi)]\left(\mathcal{H}' + 2\mathcal{H}^2\right) - \mathcal{H}\left(\Phi' + 5\Psi'\right)\right\} - (\Phi - \Psi)_{,ij}\,.
\end{aligned}
\tag{2.46}
$$

Ricci Scalar

The Ricci scalar is defined as

$$
\mathcal{R} = g^{\mu\nu} R_{\mu\nu}. \tag{2.47}
$$

And after calculation

$$
R = -\frac{2}{a^2}\left[3\Psi'' + \nabla^2(\Phi - 2\Psi) + 3\mathcal{H}\left(\Phi' + 3\Psi'\right) - 3\left(\mathcal{H}' + \mathcal{H}^2\right) + 6\Phi\left(\mathcal{H}' + \mathcal{H}^2\right)\right]. \tag{2.48}
$$

Einstein Tensor

Now the Einstein Tensor is calculated from the last results. The definition of Einstein Tensor is

$$G^{\mu}_{\nu} = R^{\mu}_{\nu} - \frac{1}{2} g^{\mu}_{\nu} \mathcal{R}. \tag{2.49}$$

Neglecting the background terms, the perturbation part of the Einstein tensor is:

$$\begin{aligned}
\delta G^0_0 &= a^{-2} \left[6\mathcal{H}\Psi' - 2\nabla^2\Psi + 6\mathcal{H}^2\Phi \right], \\
\delta G^0_i &= -2a^{-1} \left(\Psi' + \mathcal{H}\Phi \right)_{,i}, \\
\delta G^i_j &= a^{-2} \left\{ \delta_{ij} \left[\nabla^2(\Phi - \Psi) + 2\Psi'' + 2\left(2\mathcal{H}' + \mathcal{H}^2\right)\Phi + 2\mathcal{H}\left(\Phi' + 2\Psi'\right) \right] + (\Psi - \Phi)_{,ij} \right\}.
\end{aligned} \tag{2.50}$$

Equations of motion

Using the previous results and following (2.34) we can obtain explicitly three equations of motion for the perturbations. Among these equations, the ij equation immediately denotes that $\Psi = \Phi$. Then, after some algebra the resulting equations of motion are:

$$\nabla^2\Phi - 3\mathcal{H}\Phi' - \left(\mathcal{H}' + 2\mathcal{H}^2\right)\Phi = \frac{3}{2} l^2 \left(\varphi_0' \delta\varphi' + V_{,\varphi}\, a^2 \delta\varphi \right), \tag{2.51}$$

$$\Phi' + \mathcal{H}\Phi = \frac{3}{2} l^2 \varphi_0' \delta\varphi, \tag{2.52}$$

$$\Phi'' + 3\mathcal{H}\Phi' + \left(\mathcal{H}' + 2\mathcal{H}^2\right)\Phi = \frac{3}{2} l^2 \left(\varphi_0' \delta\varphi' - V_{,\varphi}\, a^2 \delta\varphi \right). \tag{2.53}$$

In these equations $l^2 = 8\pi G/3$. It is possible to combine these three equations in a single one. To do this, first (2.51) is subtracted from (2.53), and then using (2.52) and (2.9) to replace $\delta\varphi$ and $V_{,\varphi}$ respectively, one finds that

$$\Phi'' - \nabla^2\Phi + 2\left(\mathcal{H} - \frac{\varphi_0''}{\varphi_0'} \right)\Phi' + \left(2\mathcal{H}' - \frac{2\mathcal{H}\varphi_0''}{\varphi_0'} \right)\Phi = 0. \tag{2.54}$$

or this can be rewritten as

$$u'' - \nabla^2 u - z\left(\frac{1}{z}\right)'' u = 0, \tag{2.55}$$

defining $u = \frac{a}{\varphi_0'}\Phi$ and $z = \frac{a\varphi_0'}{\mathcal{H}}$. Going to Fourier space we get an equation for each k mode

$$u_{\mathbf{k}}'' + k^2 u_{\mathbf{k}} - z\left(\frac{1}{z}\right)'' u_{\mathbf{k}} = 0. \tag{2.56}$$

This equation is useful to study the evolution of perturbations when they have already crossed the horizon. But also, it is useful to find a new equation that describes the evolution of perturbations inside horizon, as next section describes.

We can calculate how perturbations are going to evolve after horizon crossing using (2.54), even without knowing its exact origin. A useful variable to study cosmological perturbations is the comoving curvature perturbation $\mathcal{R}^\dagger$, which in the longitudinal gauge is defined as:

$$\mathcal{R} = \Phi + \frac{2}{3}\frac{\Phi' + \mathcal{H}\Phi}{\mathcal{H}(1+w)}, \tag{2.57}$$

where as usual $w = p/\rho$. Combining equations (1.7) and (1.8) one finds that

$$\mathcal{H}' = -\frac{1}{2}(1+3w)\mathcal{H}^2. \tag{2.58}$$

Using equations (2.58) and (2.12), equation (2.54) can be rewritten as

$$\frac{3}{2}(1+w)\mathcal{R}' = \frac{\nabla^2}{\mathcal{H}}\Phi, \tag{2.59}$$

or in Fourier space

$$\frac{3}{2}(1+w)\mathcal{R}_{\mathrm{k}}' = -\frac{k^2}{\mathcal{H}}\Phi_k. \tag{2.60}$$

†The comoving curvature perturbation $\mathcal{R}$ is equal to the curvature perturbation Ψ in a comoving gauge.

On super-horizon scales $k << \mathcal{H}$, then the curvature perturbation $\mathcal{R}_k$ remains constant at least possibly that $1 + w = 0$, but in single field inflationary models $\mathcal{R}_k$ remains constant independently of the equation of state[19]. Thus, the curvature perturbations originates somehow during inflation inside the horizon, then they grow because of the expansion of the Universe and they will cross the horizon, at this point they will keep constant. Given that the curvature perturbation freezes in super-horizon scales, it is simpler to relate current observables with the perturbations originated during inflation, for example CMB anisotropies are directly linked with the perturbations of inflation.

2.3.2 Quantum Cosmological Perturbations

Cosmological perturbations arise from quantum vacuum fluctuations. These vacuum fluctuations originate well inside the horizon and are stretched to macroscopic levels by the expansion of the Universe. To describe this process a framework of quantum gravity is required, which is not completely established. But, measurements show that perturbations are small on large cosmological scales. For this reason, the perturbations had to be very small in the early Universe, hence the theory of cosmological perturbations at linear order is consistent to deal with this process. Mukhanov[20] first developed a consistent way to construct a gauge-invariant quantum theory of perturbations in an isotropic universe filled with a single scalar field (inflaton). In his work, he started from an action containing the usual Einstein-Hilbert action plus the action of a scalar field with a potential. Then, the longitudinal gauge is replaced in this action, keeping second order terms of the fields. Then, the action is rewritten in terms of the gauge invariant variable v (definition is bellow). Finally, after doing the quantization of the system and using variational calculus in the remaining action, the Mukhanov-Sasaki equation is obtained, which describes the evolution of perturbations completely (from sub-horizon to super-horizon scales). This procedure is lengthy, as his author mentioned, so I present a straightforward way to reach the same equation, which was presented by Durrelle et al.[21]. Following their prescriptions consider the gauge invariant quantity:

$$v = z\mathcal{R} = a\left[\delta\varphi + \frac{\varphi_0'}{\mathcal{H}}\Phi\right], \tag{2.61}$$

this variable relates with u from (2.54) by

$$v = \frac{2}{3l^2}\left(u' + \frac{z'}{z}u\right). \tag{2.62}$$

To find an equation that describes the evolution of v, we differentiate (2.62) with respect to conformal time, and then using (2.54) results in

$$\nabla^2 u = \frac{3}{2}l^2 z\left(\frac{v}{z}\right)'. \tag{2.63}$$

Taking ∇^2 of (2.54) and then inserting in (2.63) gives

$$z\left(\frac{v'' - \nabla^2 v - \frac{z''}{z}v}{z}\right)' = 0. \tag{2.64}$$

Therefore

$$v'' - \nabla^2 v - \frac{z''}{z}v = z \times C, \tag{2.65}$$

but the constant $C \neq 0$ does not describe small perturbations. For this reason C is set to 0, and the remaining terms are the Mukhanov-Sasaki equation, which in Fourier space reads

$$v_k'' + \left(k^2 - \frac{z''}{z}\right)v_k = 0. \tag{2.66}$$

In this equation $z''/z \approx H^2$, hence the horizon plays a key role in the evolution of v_k perturbations (therefore in $\mathcal{R}_k$ by definition 2.61). The time that fulfill the condition $k = aH$ is the time when the perturbation v_k crosses the Hubble horizon. In sub-horizon scales ($k \gg z''/z$), the solutions for v_k are real and imaginary oscillations with constant amplitude. On the other hand, in super-horizon scales ($k << z''/z$), $v_k \sim z$. From these results, using the definition of v, and given that z is a growing function; $\mathcal{R}_k$ undergoes damped oscillations in sub-horizon scales. Also in super-horizon scales, $\mathcal{R}_k$ keeps constant as mentioned in the previous section.

To solve the equation (2.66) the initial condition used is the Bunch-Davies vacuum

$$\lim_{-\eta\to\infty} v_{\mathrm{k}}(\eta) \to \frac{1}{\sqrt{2k}} e^{-ik\eta}. \tag{2.67}$$

For practical purposes this condition must be used when the perturbation is well inside the horizon, when v_k is in its oscillatory behavior. The power spectrum associated with v_k comes from the two point correlation function of the perturbation v, resulting in

$$\mathcal{P}_v(\eta) = |v_k(\eta)|^2 \frac{k^3}{2\pi^2}, \tag{2.68}$$

where the power spectrum depends on η and k. Using (2.61) the power spectrum for the curvature perturbation is

$$\mathcal{P}_{\mathcal{R}} = \left|\frac{1}{z} v_k\right|^2 \frac{k^3}{2\pi^2}. \tag{2.69}$$

This time the power spectrum does not depend on time because it is directly evaluated in the super-horizon scales when $\mathcal{R}_k$ reaches its constant value. For simplicity and to make contact with observations, it is a common practice to assume that the power spectrum has a power law shape. In this case, the spectrum is specified by an amplitude $A(k_*)$, and a spectral index n_s

$$\mathcal{P}_{\mathcal{R}}(k) = A\,(k_*) \left(\frac{k}{k_*}\right)^{n_s - 1}, \tag{2.70}$$

where k_* is a pivot scale at which all the quantities are evaluated. Using this definition, n_s is calculated as

$$n_{\mathrm{S}}(k) - 1 = \frac{\mathrm{d}\ln \mathcal{P}_{\mathcal{R}}}{\mathrm{d}\ln k}. \tag{2.71}$$

Also, to allow a mildly scale-dependent power spectrum, a "running" for the spectral index is introduced, it is defined as

$$\alpha_{\mathrm{S}}(k) = \frac{\mathrm{d}n_{\mathrm{S}}}{\mathrm{d}\ln k}. \tag{2.72}$$

The power spectrum is a critical function in inflation because it is used to prove the truthfulness of any inflationary model, comparing it with measurements. Mukhanov-Sasaki equation must be solved to determine the power spectrum, but this is not a trivial task. In fact, Mukhanov-Sasaki equation is of the same type as Schrdinger equation, which happened to be difficult to solve, even for simple models. Exact analytic solutions are not available for most of the inflationary models. Then, several approximation methods are used such as slow-roll, constant-horizon, and growing-horizon [22]. On the other hand, Mukhanov-Sasaki equation can be solved numerically mode by mode as next sections describe.

2.4 Models of Inflation

2.4.1 Chaotic Inflation

Potentials of the type $V \propto \varphi^{\alpha}$ are called chaotic or power law models. Although this type of models are now strongly disfavoured by Planck 2018 [11], they are useful because of their simplicity. The inflationary model used in this work is

$$V(\varphi) = \frac{1}{2}m^2\varphi^2, \tag{2.73}$$

where m is the mass of the field. It is worth to mention that the first slow-roll parameter (2.24) for this model is

$$\epsilon = \frac{2M_{Pl}^2}{\varphi_0^2}. \tag{2.74}$$

Given that $\epsilon = 1$ marks the end of inflation, for this model the end of inflation occurs when $\varphi_0 = \sqrt{2}M_{Pl}$.

To calculate the power spectrum of scalar perturbations first the background dynamics must be solved. The scale factor and the background of the inflaton are calculated from equations (2.8) and (2.9), for this model these equations are:

$$\left(\frac{\dot{a}}{a}\right)^2 = H^2 = \frac{1}{6M_{pl}^2}(m^2\varphi_0^2 + \dot{\varphi_0}^2), \tag{2.75}$$

$$\ddot{\varphi}_0 + 3H\dot{\varphi}_0 + m^2\varphi_0 = 0. \tag{2.76}$$

Three initial conditions are required to solve this system of differential equations, but slow-roll approximation is employed to lower the number of initial condition to two. The variables a and φ_0 have the following solutions in the slow-roll approximation for the chaotic model under discussion:

$$\varphi_0(t) = \varphi_{0i} - mM_{Pl}\sqrt{\frac{2}{3}}t, \tag{2.77}$$

$$a(t) = a_i exp\left[\frac{m\varphi_{0i}}{\sqrt{6}M_{Pl}}t - \frac{m^2}{6}t^2\right]. \tag{2.78}$$

These two remaining initial conditions are specified in the next section. Once slow-roll solutions are found, they serve as initial conditions to the equations (2.75) and (2.76). Then, with the solutions of the background dynamics we can solve numerically the Mukhanov-Sasaki equation mode by mode, to finally calculate the power spectrum of scalar perturbations through (2.69).

Chapter 3

Results & Discussion

The numerical results of this section are divided in three parts, background evolution, perturbations evolution, and the power spectrum, all these results belong to inflationary model $\frac{1}{2}m^2\varphi^2$. The first section shows the evolution of the background variables a and φ_0. The second section shows the evolution of the perturbations resulting from Mukhanov-Sasaki equation. The last section presents the power spectrum with its spectral index and running. All the results presented bellow were computed in a usual laptop with a CPU Core i7 using the software Mathematica 12.0[23].

3.1 Background dynamics

The dynamics of the scale factor a and the background of the inflaton field φ_0 is found by solving the differential equations (2.75) and (2.76). As mentioned in the last section, two remaining initial conditions are required to solve the system. There is some freedom choosing these initial conditions given that a wide range of initial conditions undergoes an attractor trajectory[24 25]. The main requirement for the initial conditions is that they must provide enough inflation to solve the flatness and horizon problems. Taking as reference the work of Swagat et al.[26], I set $m = 5.97 \times 10^{-6}$, and $a(0) = 1$; also two different initial conditions are considered for the background inflaton $\varphi_0(0)$, one positive $\varphi_1 = 17$, and one negative $\varphi_2 = -17$. The code to obtain the following results is presented in Appendix A. The results of a and φ_0 are presented in the in Figure 3.1 and 3.2 respectively. The solutions for the different initial conditions end in a very similar dynamics, which is due to the attractor property of the system. Figure 3.1 shows that the scale factor is increasing like an exponential function during inflation, which guarantees that the Universe is expanding with a positive acceleration. Meanwhile, Figure 3.2 shows that the inflaton field is rolling the potential during inflation, and it starts to oscillate as soon as inflation ends. The time when inflation ends t_{end}, which corresponds to the time when $\epsilon = 1$ from (2.74), is presented in Table 3.1.

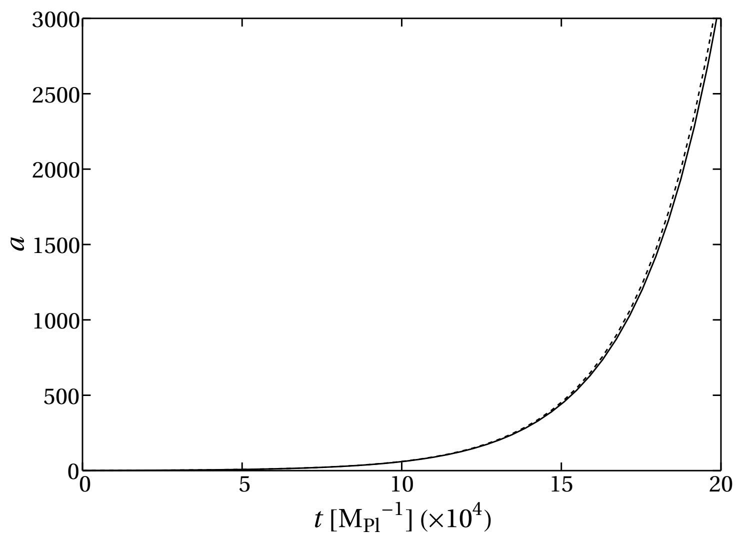

Figure 3.1: Evolution of the scale factor a for the chaotic inflationary model $\frac{1}{2}m^2\varphi_0^2$. Solid line corresponds with the initial condition $\varphi_1 = 17$, and dashed line corresponds with the initial condition $\varphi_2 = -17$.

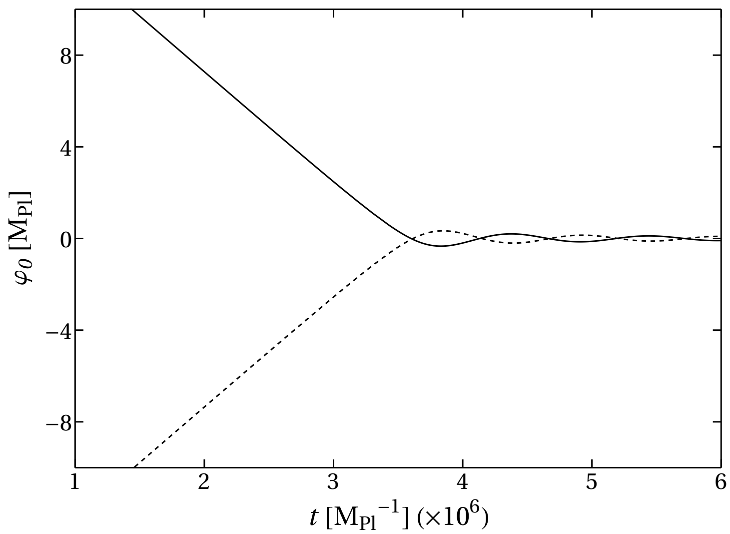

Figure 3.2: Evolution of the background inflaton field φ_0 for the chaotic inflationary model $\frac{1}{2}m^2\varphi_0^2$. Solid line corresponds with the initial condition $\varphi_1 = 17$, and dashed line corresponds with the initial condition $\varphi_2 = -17$.

Table 3.1: Time at the end of inflation t_{end} and number of e-foldings N obtained for the chaotic inflationary model $\frac{1}{2}m^2\varphi^2$ for two different initial conditions.

Initial Condition	t_{end} $[M_{Pl}^{-1}]$	N (since $t = 0$)
$\varphi_1 = 17$	3.23×10^6	72.51
$\varphi_2 = -17$	3.25×10^6	73.18

3.2 Perturbations dynamics

The evolution of perturbations is determined by the Mukhanov-Sasaki equation (2.66). This equation is solved using physical time t as independent variable, whence transforming the equation to the time domain (using $dt = ad\eta$), gives:

$$\ddot{v}_k + \dot{v}_k H + v_k \left[\frac{k^2}{a^2} - \frac{1}{az} \left(\dot{a}\dot{z} + a\ddot{z} \right) \right] = 0. \tag{3.1}$$

The relation between t and η is computed to apply the initial condition (2.67) to this equation. Figure 3.3 shows $\eta(t)$ for $\varphi_1 = 17$, it is calculated by numerical integration of $\eta(t) = \int_0^t \frac{dt'}{a(t')}$ and imposing that $\eta(t_{end}) = 0$ (this condition is usual in works on inflation).

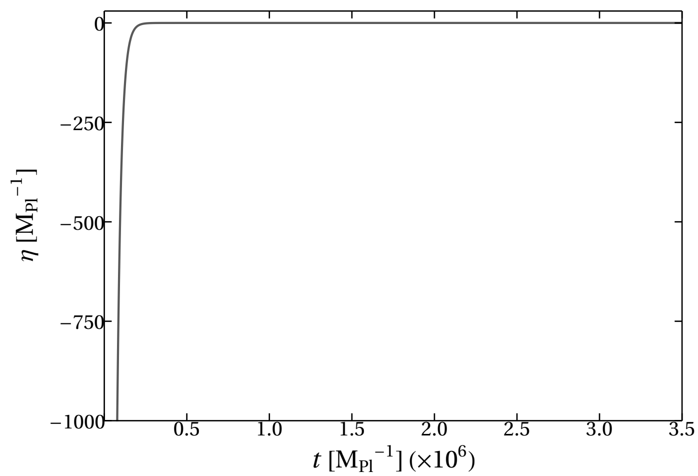

Figure 3.3: Behavior of conformal time η as a function of physical time t for the chaotic inflationary model $\frac{1}{2}m^2\varphi_0^2$ for the initial condition $\varphi_1 = 17$.

To properly apply the initial condition (2.67) well inside the horizon, equation (3.1) is break into two regimes. First, the sub-horizon regime where $k \gg z''/z$, hence the term z''/z is neglected. Second, a regime where the full equation is considered. The first regime is used to impose the initial condition at a time that corresponds to approximately 300 oscillations before horizon crossing (the number of oscillations n from a time t to the horizon crossing time t_{hc} for a mode k is given by $\pi n = k\left[\eta(t_{hc}) - \eta(t)\right]$). Then, the result of this first regime serves as initial condition to the second regime at 100 oscillations before horizon crossing. The code to find the following results is presented in Appendix B. The real and imaginary parts of the perturbation v_k for the mode $k = 0.05$ are plotted in Figure (3.4) and (3.5) respectively. The perturbation undergoes almost the same dynamics independently of the initial condition. As previously discussed, the perturbation has an oscillatory behavior inside the horizon, and grows indefinitely after the horizon crossing.

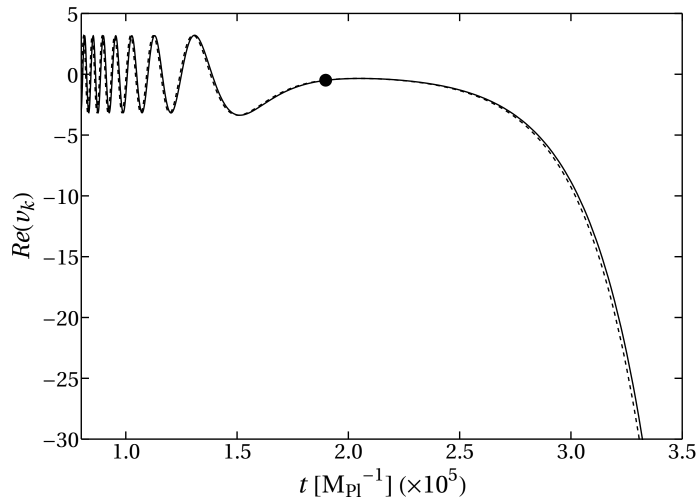

Figure 3.4: Re(v_k) versus physical time for the chaotic inflationary model $\frac{1}{2}m^2\varphi_0^2$ for the mode $k = 0.05$. Highlighted point represents the moment when the perturbations cross the horizon. Solid line corresponds with the initial condition $\varphi_1 = 17$, and dashed line corresponds with the initial condition $\varphi_2 = -17$.

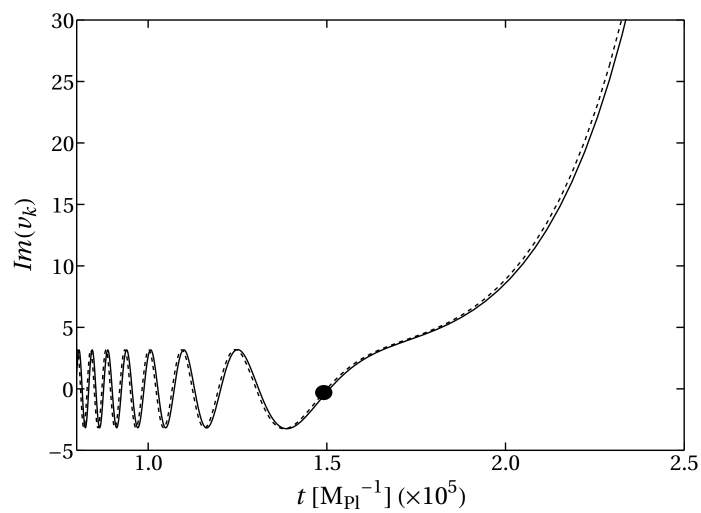

Figure 3.5: Im(v_k) versus physical time for the chaotic inflationary model $\frac{1}{2}m^2\varphi_0^2$ for the mode $k = 0.05$. Highlighted point represents the moment when the perturbations cross the horizon. Solid line corresponds with the initial condition $\varphi_1 = 17$, and dashed line corresponds with the initial condition $\varphi_2 = -17$.

Also, it is interesting to see the behavior of the curvature perturbation $\mathcal{R}$ for the same $k = 0.05$. Figures (3.6) and (3.7) show the dynamics of the real and imaginary part of the curvature perturbation respectively. Figure (3.6) shows that Re($\mathcal{R}$) converges to the same value, after horizon crossing, no matter the initial condition. Figure (3.7) apparently shows that Im($\mathcal{R}$) does not converge to the same value, but for the power spectrum just the quantity $|\mathcal{R}|$ is relevant. In Figure (3.8) we see that the power spectrum converges to the same value regardless of the initial condition.

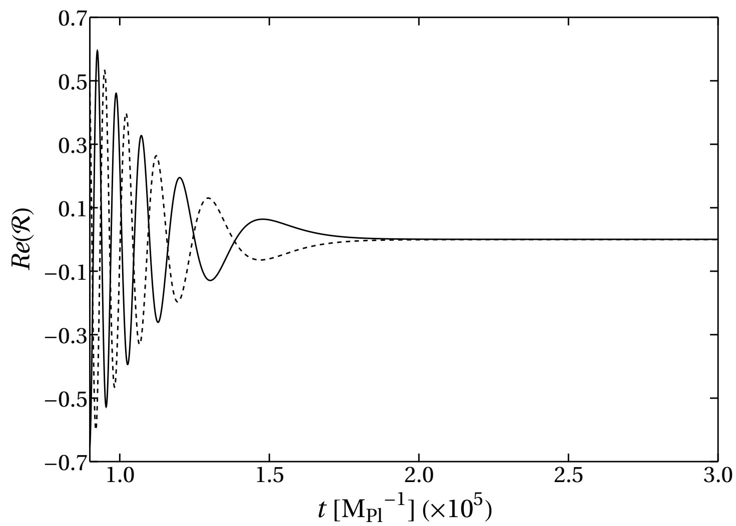

Figure 3.6: Re($\mathcal{R}$) versus physical time for the chaotic inflationary model $\frac{1}{2}m^2\varphi_0^2$ for the mode $k = 0.05$. Solid line corresponds with the initial condition $\varphi_1 = 17$, and dashed line corresponds with the initial condition $\varphi_2 = -17$.

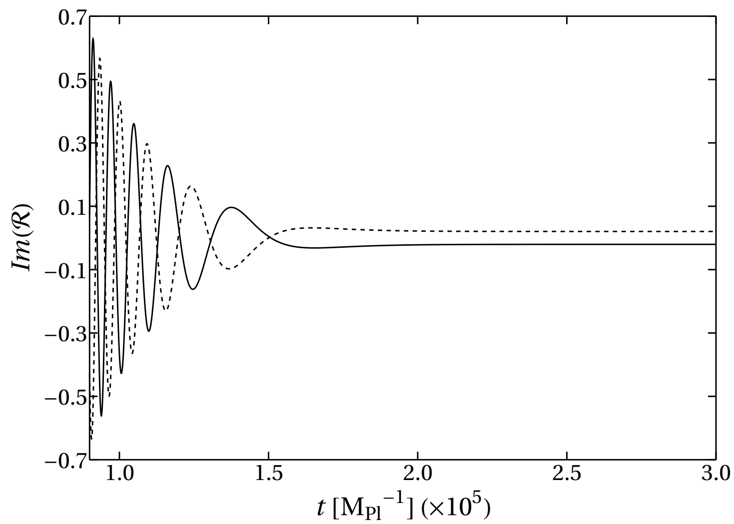

Figure 3.7: Im($\mathcal{R}$) versus physical time for the chaotic inflationary model $\frac{1}{2}m^2\varphi_0^2$ for the mode $k = 0.05$. Solid line corresponds with the initial condition $\varphi_1 = 17$, and dashed line corresponds with the initial condition $\varphi_2 = -17$.

3.3 Power Spectrum

Once the perturbations v_k are determined, the power spectrum can be computed from equation (2.69). Figure (3.8) shows the dynamics of the power spectrum for the mode $k = 0.05$, the spectrum presents its asymptotic behavior from $t \approx 2 \times 10^5 M_{Pl}^{-1}$ on. Considering this, the evaluation of the power spectrum for all k modes is done at $t = 1 \times 10^6 M_{Pl}^{-1}$, hence there is enough time for the spectrum to converge. Figure (3.9) shows the main result of this thesis, the power spectrum of scalar perturbations for chaotic inflation $\frac{1}{2}m^2\varphi_0^2$ for different k modes. The points for the smallest k modes seem to deviate from the main linear tendency (in semi-log scale). This is an evidence that the numerical calculation has some problems at small k values. The problem could be that the Bunch-Davies initial condition must be applied when $k\eta \to -\infty$, but numerically this can be difficult to achieve for small k values. To circumvent these problems further approximations must be applied such as the uniform approximation[27], or phase-integral approximation[28]. Despite of this issue, the majority of the power spectrum seems to be smooth, therefore it is possible to extract consistently the spectral index and running, through numerical differentiation, using their definitions in equation (2.71) and (2.72). Table (3.2) presents the values of n_s and α_s for the two initial conditions and the values reported by Planck 2018 results. X. Constraints on inflation[1]. Although the chaotic model studied is a simple model, the spectral index predicted is really close to the current measurements. In fact the spectral index for the initial condition $\varphi_1 = 17$ lies inside the interval reported by Planck 2018.

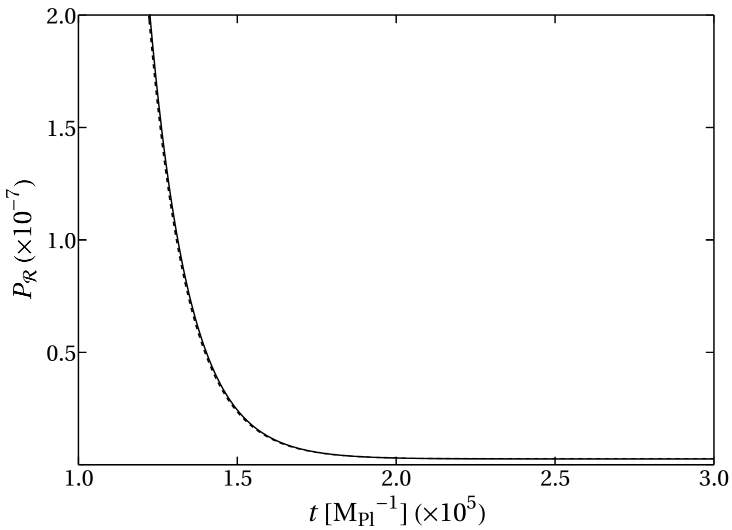

Figure 3.8: Evolution of the power spectrum for the chaotic inflationary model $\frac{1}{2}m^2\varphi_0^2$ for the mode $k = 0.05$. Solid line corresponds with the initial condition $\varphi_1 = 17$, and dashed line corresponds with the initial condition $\varphi_2 = -17$.

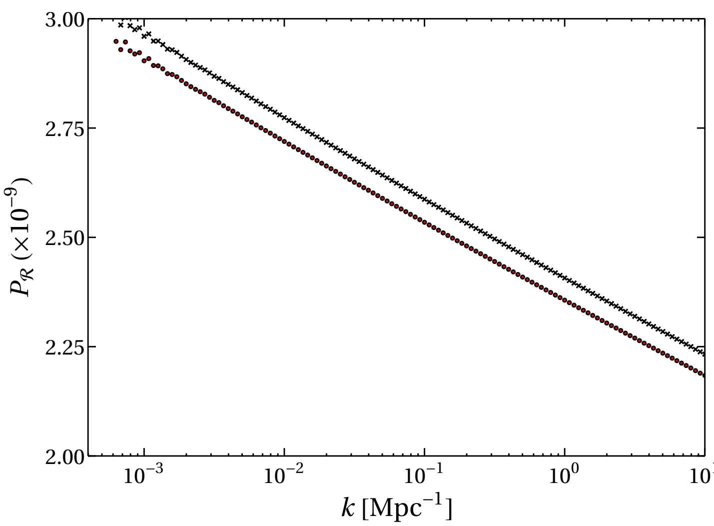

Figure 3.9: The power spectrum of scalar perturbations for the chaotic inflationary model $\frac{1}{2}m^2\varphi_0^2$. Red dots correspond with the initial condition $\varphi_1 = 17$, and black crosses correspond with the initial condition $\varphi_2 = -17$.

Table 3.2: Values of n_s and α_s obtained by numerical computation with two initial conditions for the chaotic inflationary model $\frac{1}{2}m^2\varphi_0^2$ for $k = 0.05$, and the measurements reported in Planck 2018 results. X. Constraints on inflation[1].

	Computation with $\varphi_1 = 17$	Computation with $\varphi_2 = -17$	Measurement (68% CL)
n_s	0.9689	0.9696	0.9649 ± 0.0042
α_s	−0.0311	−0.0304	−0.0045 ± 0.0067

Chapter 4

Conclusions & Outlook

In this work a brief introduction to inflation and cosmological perturbations was presented, starting with the fine-tuning problems, which were the first motivation to bring in cosmological inflation. Then, the dynamics of the Universe during an inflationary epoch was presented, accompanied with the slow-roll approximation. Cosmological Perturbations were discussed in their classical and quantum treatments, ending with the Mukhanov-Sasaki equation and its direct relation with the power spectrum of scalar perturbations. The background and perturbations dynamics of the chaotic inflationary model $\frac{1}{2}m^2\varphi^2$ were presented, and they showed that two different initial conditions lead to almost the same dynamics, as evidence of the attractor behavior of the system. The power spectrum of scalar perturbation for chaotic inflation is presented in Figure 3.9, and its corresponding spectral index is in good agreement with the results reported by Planck 2018 results. X[1]. Constraints on inflation, as Table 3.2 shows.

For future developments, the calculation of the power spectrum could be computed under different numerical methods to get more accurate results. Also, more computational power can be used to calculate the spectrum. About the small k problem of the power spectrum briefly mentioned, different approximations should be tested to compensate this problem. More initial conditions coming from a wide range could be used to remake all the calculations to proof the limits of the attractor in the system, but also to test how different initial conditions affect the resulting power spectrum. Moreover, the code described in this work can be extended to calculate the power spectrum of tensor perturbations. An important future work is to use the code presented in this work to calculate the power spectrum of scalar perturbations of more favored by data models, such as Starobinsky inflation[29].

Appendix A

Mathematica code to calculate the background dynamics

$$
\begin{aligned}
m &:= \frac{597}{100000000} \\
c &= 17 \\
w &= \mathrm{NDSolve}\Big[\left\{\frac{3\phi\mathrm{t}'[t]\sqrt{m^2\phi\mathrm{t}[t]^2+\phi\mathrm{t}'[t]^2}}{\sqrt{6}}+m^2\phi\mathrm{t}[t]+\phi\mathrm{t}''[t]=0, \phi\mathrm{t}[0]=c, \phi\mathrm{t}'[0]=-\frac{\sqrt{6}m}{3}\right\} \\
, &\quad \left\{\phi\mathrm{t}, \phi\mathrm{t}', \phi\mathrm{t}'', \phi\mathrm{t}^{(3)}\right\}, \{t, 0, 3\times 10^7\}, \mathrm{AccuracyGoal}\to 10, \mathrm{PrecisionGoal}\to\infty \\
, &\quad \mathrm{WorkingPrecision}\to 15, \mathrm{StartingStepSize}\to 0.00001, \mathrm{MaxStepSize}\to 200 \\
, &\quad \mathrm{Null}, \mathrm{MaxSteps}\to\infty, \mathrm{InterpolationOrder}\to\mathrm{All}\Big]; \\
\phi[\mathrm{t\_}] &:= (\phi\mathrm{t}/.\,\mathrm{First}[w])[t]; \\
\mathrm{d} &= \mathrm{NDSolve}\Big[\left\{\frac{\mathrm{at}'[t]}{\mathrm{at}[t]}=\frac{\sqrt{m^2\phi[t]^2+\mathrm{p}\phi[t]^2}}{\sqrt{6}}, \mathrm{at}[0]=1\right\}, \left\{\mathrm{at}, \mathrm{at}', \mathrm{at}'', \mathrm{at}^{(3)}\right\}, \{t, 0, 3\times 10^7\} \\
, &\quad \mathrm{AccuracyGoal}\to 10, \mathrm{PrecisionGoal}\to 10, \mathrm{WorkingPrecision}\to 15, \mathrm{StartingStepSize}\to 0.0001 \\
, &\quad \mathrm{MaxStepSize}\to 200, \mathrm{MaxSteps}\to\infty, \mathrm{InterpolationOrder}\to\mathrm{All}\Big]; \\
a[\mathrm{t\_}] &:= (\mathrm{at}/.\,\mathrm{First}[\mathrm{d}])[t];
\end{aligned}
$$

Appendix B

Mathematica code to calculate the perturbation dynamics

This code works once the code in appendix A is run previously. First, the calculation of the conformal time η:

$$\text{conformal} = \text{NDSolve}\left[\left\{\text{conf}'[t] = \frac{1}{a[t]}, \text{conf}[\text{tend}] = 0\right\}, \{\text{conf}, \text{conf}'\}, \{t, 0, 30000000\}\right.$$

$$, \quad \text{AccuracyGoal} \to 10, \text{PrecisionGoal} \to 10, \text{WorkingPrecision} \to 15, \text{MaxSteps} \to \infty$$

$$, \quad \left.\text{InterpolationOrder} \to \text{All}\right];$$

$$\eta[\text{t\_}] \quad := (\text{conf}/.\,\text{First}[\text{conformal}])[t];$$

$$\text{p}\eta[\text{t\_}] \quad := (\text{conf}'/.\,\text{First}[\text{conformal}])\,[t];$$

Then, defining the components of Mukhanov-Sasaki equation:

$$
\begin{aligned}
&\mathrm{p}\phi[\mathrm{t\_}] &&:= (\phi\mathrm{t}' /.\ \mathrm{First}[w])\,[t];\\
&\mathrm{pa}[\mathrm{t\_}] &&:= (\mathrm{at}' /.\ \mathrm{First}[\mathrm{ww}])\,[t];\\
&\mathrm{ppa}[\mathrm{t\_}] &&:= (\mathrm{at}'' /.\ \mathrm{First}[\mathrm{ww}])\,[t];\\
&\mathrm{pppa}[\mathrm{t\_}] &&:= \left(\mathrm{at}^{(3)} /.\ \mathrm{First}[\mathrm{ww}]\right)[t];\\
&z[\mathrm{t\_}] &&:= \frac{a[t]^2\mathrm{p}\phi[t]}{\mathrm{pa}[t]};
\end{aligned}
$$

$$
\begin{aligned}
&\mathrm{pz}[\mathrm{t\_}] &&:= a[t]\left(\mathrm{p}\phi[t]\left(2-\frac{a[t]\mathrm{ppa}[t]}{\mathrm{pa}[t]^2}\right)+\frac{a[t]\mathrm{pp}\phi[t]}{\mathrm{pa}[t]}\right)\\
&\mathrm{ppz}[\mathrm{t\_}] &&:= -\frac{a[t]^2(2\mathrm{ppa}[t]\mathrm{pp}\phi[t]+\mathrm{pppa}[t]\mathrm{p}\phi[t])}{\mathrm{pa}[t]^2}+\frac{a[t](a[t]\mathrm{ppp}\phi[t]-2\mathrm{ppa}[t]\mathrm{p}\phi[t])}{\mathrm{pa}[t]}\\
&+ && \frac{2a[t]^2\mathrm{ppa}[t]^2\mathrm{p}\phi[t]}{\mathrm{pa}[t]^3}+4a[t]\mathrm{pp}\phi[t]+2\mathrm{pa}[t]\mathrm{p}\phi[t]\\
&\mathrm{rhs}[\mathrm{k\_},\mathrm{t\_}] &&:= \frac{1}{a[t]^2}\left(k^2-\frac{a[t](a[t]\mathrm{ppz}[t]+\mathrm{pa}[t]\mathrm{pz}[t])}{z[t]}\right);
\end{aligned}
$$

Defining the initial condition:

$$
\begin{aligned}
&\mathrm{uini}[\mathrm{k\_},\mathrm{t\_}] &&:= \mathrm{Rationalize}\left[\frac{\exp(-ik\eta[t])}{\sqrt{2k}},0\right];\\
&\mathrm{difuini}[\mathrm{k\_},\mathrm{t\_}] &&:= \mathrm{Rationalize}\left[-\frac{(ik\mathrm{p}\eta[t])\exp(-ik\eta[t])}{\sqrt{2k}},0\right];
\end{aligned}
$$

Finding the initialization time for the two regimes of Mukhanov-Sasaki equation:

$$\begin{aligned}
\text{hc[k_]} &:= \text{Rationalize}\left[\text{FindRoot}\left[k - \text{pa}[t], \left\{t, 10^4 k, 10^5 k\right\}\right][[1,2]], 0\right];\\
\text{nzeros[k_]} &:= n/.\,\text{First}\left[\text{NSolve}\left[n = \frac{k(\eta[\text{hc}[k]] - \eta[0])}{\pi}, n, \text{WorkingPrecision} \to 15\right]\right]\\
\text{etabuch[k_]} &:= \text{NSolve}[k(\eta[\text{hc}[k]] - \text{eta}) = 300\pi, \text{eta}]\\
\text{etaini[k_]} &:= \text{NSolve}[k(\eta[\text{hc}[k]] - \text{eta}) = 100\pi, \text{eta}]\\
\text{suptbuch[k_]} &:= \text{FindRoot}[\eta[t] = (\text{eta}/.\,\text{First}[\text{etabuch}[k]]), \{t, 5000k, 50000k\}][[1,2]]\\
\text{suptini[k_]} &:= \text{FindRoot}[\eta[t] = (\text{eta}/.\,\text{First}[\text{etaini}[k]]), \{t, 5000k, 50000k\}][[1,2]]\\
\text{tbuch[k_]} &:= \text{Piecewise}[\{\{\text{hc}[k] \times 0.0001, k \le 0.06\}, \{\mathit{suptbuch}[k], k > 0.06\}\}]\\
\text{tini[k_]} &:= \text{Piecewise}[\{\{\text{hc}[k] \times 0.05, k \le 0.06\}, \{\mathit{suptbuch}[k], k > 0.06\}\}]
\end{aligned}$$

Solving the Mukhanov-Sasaqui equation

$$\begin{aligned}
\text{prere[k_]} := \text{NDSolve}\Big[&\{l[t]\left(\frac{k}{a[t]}\right)^2 + H[t]l'[t] + l''[t] = 0, l[\text{tbuch}[k]] = \text{Re}[\text{uini}[k, \text{tbuch}[k]]]\\
,\quad & l'[\text{tbuch}[k]] = \text{Re}[\text{difuini}[k, \text{tbuch}[k]]]\}, \{l, l'\}, \{t, \text{tbuch}[k], \text{tini}[k]\}, \text{MaxSteps} \to \infty\\
,\quad & \text{StartingStepSize} \to 0.0001, \text{MaxStepSize} \to 10, \text{InterpolationOrder} \to \text{All}\Big];
\end{aligned}$$

$$
\begin{aligned}
\text{re[k\_]} \quad &:= \text{NDSolve}\Big[\{u[t]\text{rhs}[k,t] + H[t]u'[t] + u''[t] = 0, u[\text{tini}[k]] \\
= \quad & \text{Rationalize}[(l/.\,\text{First}[\text{prere}[k]])[\text{tini}[k]], 0], u'[\text{tini}[k]] \\
= \quad & \text{Rationalize}\,[(l'/.\,\text{First}[\text{prere}[k]])\,[\text{tini}[k]], 0]\,\}, u, \{t, \text{tini}[k], 1000000\}, \text{MaxSteps} \to \infty \\
, \quad & \text{StartingStepSize} \to 0.001, \text{MaxStepSize} \to 10, \text{InterpolationOrder} \to \text{All}\Big]; \\
\text{preim[k\_]} \quad &:= \text{NDSolve}\Big[\{g[t]\left(\frac{k}{a[t]}\right)^2 + H[t]g'[t] + g''[t] = 0, g[\text{tbuch}[k]] = \text{Im}[\text{uini}[k], \text{tbuch}[k]]] \\
, \quad & g'[\text{tbuch}[k]] = \text{Im}[\text{difuini}[k, \text{tbuch}[k]]]\}, \{g, g'\}, \{t, \text{tbuch}[k], \text{tini}[k]\}, \text{MaxSteps} \to \infty \\
, \quad & \text{StartingStepSize} \to 0.0001, \text{MaxStepSize} \to 10, \text{InterpolationOrder} \to \text{All}\Big]; \\
\text{im[k\_]} \quad &:= \text{NDSolve}\Big[\{v[t]\text{rhs}[k,t] + H[t]v'[t] + v''[t] = 0, v[\text{tini}[k]] \\
= \quad & \text{Rationalize}[(g/.\,\text{First}[\text{prere}[k]])[\text{tini}[k]], 0], v'[\text{tini}[k]] \\
= \quad & \text{Rationalize}\,[(g'/.\,\text{First}[\text{prere}[k])\,[\text{tini}[k]], 0]\,\}, v, \{t, \text{tini}[k], 1000000\}, \text{MaxSteps} \to \infty \\
, \quad & \text{StartingStepSize} \to 0.001, \text{MaxStepSize} \to 10, \text{InterpolationOrder} \to \text{All}\Big];
\end{aligned}
$$

Bibliography

[1] Akrami, Y.; Arroja, E.; Ashdown, M.; Aumont, J.; Calabrese, E. Planck 2018 results. X. Constraints on inflation. *Astronomy and Astrophysics* **2019**,

[2] Choquet-Bruhat, Y. *Introduction to general relativity, black holes, and cosmology*; OUP Oxford, 2014.

[3] Weinberg, S. *Gravitation and cosmology: principles and applications of the general theory of relativity*; Wiley New York, 1973.

[4] Bucher, M. Physics of the cosmic microwave background anisotropy. *International Journal of Modern Physics D* **2015**, *24*, 1530004.

[5] Guth, A. H. Inflationary universe: A possible solution to the horizon and flatness problems. *Physical Review D* **1981**, *23*, 347.

[6] Mukhanov, V. F.; Chibisov, G. Quantum fluctuations and a nonsingular universe. *JETP Lett.* **1981**, *33*, 532–535.

[7] Mukhanov, V. F.; Chibisov, G. Vacuum energy and large-scale structure of the universe. *Soviet Physics-JETP* **1982**, *56*, 258–265.

[8] Martin, J.; Ringeval, C.; Trotta, R.; Vennin, V. The best inflationary models after Planck. *Journal of Cosmology and Astroparticle Physics* **2014**, *2014*, 039.

[9] Bennett, C. First Year WMAP Observations. *Maps of the Cosmos* **2005**, *216*, 18.

[10] Boggess, N.; Mather, J.; Weiss, R.; Bennett, C.; Cheng, E. a.; Dwek, E.; Gulkis, S.; Hauser, M.; Janssen, M.; Kelsall, T. The COBE mission-Its design and performance two years after launch. *The Astrophysical Journal* **1992**, *397*, 420–429.

[11] Aghanim, N.; Akrami, Y.; Ashdown, M.; Aumont, J.; Baccigalupi, C.; Ballardini, M.; Banday, A.; Barreiro, R.; Bartolo, N.; Basak, S. Planck 2018 results. VI. Cosmological parameters. *arXiv preprint arXiv:1807.06209* **2018**,

[12] Martin, J. Cosmic Inflation: Trick or Treat? *arXiv preprint arXiv:1902.05286* **2019**,

[13] Liddle, A. R.; Lyth, D. H. *Cosmological inflation and large-scale structure*; Cambridge University Press, 2000.

[14] Davis, T. M.; Lineweaver, C. H. Expanding Confusion: common misconceptions of cosmological horizons and the superluminal expansion of the Universe. *Publications of the Astronomical Society of Australia* **2004**, *21*, 97–109.

[15] Patel, V. M.; Lineweaver, C. H. Solutions to the Cosmic Initial Entropy Problem without Equilibrium Initial Conditions. *Entropy* **2017**, *19*, 411.

[16] Bardeen, J. M. Gauge-invariant cosmological perturbations. *Physical Review D* **1980**, *22*, 1882.

[17] Mukhanov, V. F.; Feldman, H. A.; Brandenberger, R. H. Theory of cosmological perturbations. *Physics reports* **1992**, *215*, 203–333.

[18] Brandenberger, R. H. *The Early Universe and Observational Cosmology*; Springer, 2004; pp 127–167.

[19] Lin, W.; Meng, X.; Zhang, X. Adiabatic gravitational perturbation during reheating. *Physical Review D* **2000**, *61*, 121301.

[20] Mukhanov, V. F. Quantum theory of gauge-invariant cosmological perturbations. *Zh. Eksp. Teor. Fiz* **1988**, *94*.

[21] Deruelle, N.; Gundlach, C.; Polarski, D. On the quantization of perturbations in inflation. *Classical and Quantum Gravity* **1992**, *9*, 137–148.

[22] Schwarz, D. J.; Terrero-Escalante, C. A. Primordial fluctuations and cosmological inflation after WMAP 1.0. *Journal of Cosmology and Astroparticle Physics* **2004**, *2004*, 003.

[23] Wolfram Research, I. Mathematica, Versión 12.1. `https://www.wolfram.com/mathematica`, Champaign, IL, 2020.

[24] Belinsky, V.; Ishihara, H.; Khalatnikov, I.; Sato, H. On the degree of generality of inflation in Friedmann cosmological models with a massive scalar field. *Progress of Theoretical Physics* **1988**, *79*, 676–684.

[25] Belinsky, V.; Grishchuk, L.; Khalatnikov, I.; Zeldovich, Y. Inflationary stages in cosmological models with a scalar field. *Physics Letters B* **1985**, *155*, 232 – 236.

[26] Mishra, S. S.; Sahni, V.; Toporensky, A. V. Initial conditions for inflation in an FRW universe. *Physical Review D* **2018**, *98*, 083538.

[27] Habib, S.; Heinen, A.; Heitmann, K.; Jungman, G. Inflationary perturbations and precision cosmology. *Physical Review D* **2005**, *71*, 043518.

[28] Rojas, C.; Villalba, V. M. Computation of inflationary cosmological perturbations in chaotic inflationary scenarios using the phase-integral method. *Physical Review D* **2009**, *79*, 103502.

[29] Starobinsky, A. A. *30 Years Of The Landau Institute—Selected Papers*; World Scientific, 1996; pp 771–774.

Abbreviations

BBN Big Bang Nucleosynthesis 9

CMB Cosmic Microwave Background 1, 2, 5–7

FLRW Friedmann-Lamaıtre-Robertson-Walker 2

GUT Grand Unified Theory 15